phys. stat. sol. (a) **49**, 629 (1978)

Subject classification: 1.5; 13.4; 14.3.1; 20.1; 20.3; 22.2.4

Zentralinstitut für Elektronenphysik der Akademie der Wissenschaften der DDR, Berlin (a), Lebedev-Institut, Moskau (b), and Sektion Physik der Karl-Marx-Universität, Leipzig (c)

Growth and Properties of $Al_xGa_{1-x}N$ Epitaxial Layers

By

B. BARANOV (a), L. DÄWERITZ (a), V. B. GUTAN (b), G. JUNGK (a), H. NEUMANN (c), and H. RAIDT (a)

$Al_xGa_{1-x}N$ layers up to $x = 0.45$ are grown on sapphire substrates with different orientations via vapour phase reaction of NH_3 with the chlorides of Ga and Al. Epitaxial growth with good crystalline perfection is observed on (0001)- and (1$\bar{1}$02)-oriented substrates. Indications to the existence of a cubic sphalerite phase in $Al_xGa_{1-x}N$ are found. All undoped layers are n-type conducting with electron concentrations above 10^{19} cm^{-3} and show a tendency to lower electron concentrations with rising x. The electron mobility depends strongly on the growth conditions. Optical transmission measurements show the expected increase of the band gap with x. Photoluminescence spectra of undoped layers are dominated by a structure near 3.46 eV independent of x. Some results for Zn-doped samples are also given.

$Al_xGa_{1-x}N$-Schichten bis zu $x = 0{,}45$ werden auf Saphirsubstraten unterschiedlicher Orientierung über die Gasphasenreaktion von NH_3 mit den Chloriden des Ga und Al abgeschieden. Epitaktisches Wachstum mit guter Kristallperfektion ergibt sich auf (0001)- und (1$\bar{1}$02)-orientierten Substraten. Es werden Hinweise auf die Existenz einer kubischen Sphaleritphase in $Al_xGa_{1-x}N$ gefunden. Alle Schichten sind n-leitend mit Elektronenkonzentrationen oberhalb 10^{19} cm^{-3} und zeigen eine Tendenz zu niedrigeren Elektronenkonzentrationen mit wachsendem x. Die Elektronenbeweglichkeit hängt stark von den Züchtungsbedingungen ab. Optische Transmissionsmessungen zeigen den erwarteten Anstieg in der Breite der verbotenen Zone mit wachsendem x. Photolumineszenzspektren undotierter Schichten werden von einer Struktur nahe 3,46 eV beherrscht, die unabhängig von x ist. Einige Ergebnisse für Zn-dotierte Proben werden ebenfalls mitgeteilt.

1. Introduction

The semiconducting III–V compound GaN has a large direct energy gap, can be an efficient light emitter over a wide spectral range including the visible and ultraviolet, and has been made to lase in the ultraviolet [1]. However, this potential usefulness of GaN for optoelectronic applications appears to be limited by the fact that amphoteric doping has not been achieved under equilibrium conditions, probably due to the effect of vacancy self-compensation [2, 3]. A promising possibility to overcome the difficulty in the preparation of p-type material seems to be the admixture of AlN to GaN. Low-resistivity AlN with n- as well as p-type conduction can be prepared by suitable doping [4] and evidence for an effective ultraviolet dc electroluminescence of AlN has been also given in the literature [5]. Thus, it might be possible to get n- and p-type $Al_xGa_{1-x}N$ crystals and an effective radiative recombination in the visible as well as ultraviolet above some critical Al content of the mixed crystal system.

The present communication contains a brief description of the preparation of $Al_xGa_{1-x}N$ epitaxial layers and reports some results concerning the structural, electrical, and optical properties of the layers.

2. Experimental

2.1 Sample preparation

The growth apparatus used for the preparation of the $Al_xGa_{1-x}N$ layers is similar to that previously developed for the epitaxial growth of GaN with some modifications as described in [6, 7]. The layers were grown on sapphire substrates with orientations (0001), (1$\bar{1}$02), (10$\bar{1}$0), and ($\bar{1}$011) at a temperature of about 1050 °C via vapour phase reaction of NH_3 with chlorides of gallium and aluminium in a nitrogen carrier gas ambient. Some remarks are necessary concerning the chemical transport reactions involved in the deposition of $Al_xGa_{1-x}N$. According to [8] there exist two thermodynamically feasible reactions which lead to the deposition of GaN. Under usual growth conditions the largest contribution comes from the reaction [8, 9]

$$GaCl + NH_3 \rightarrow GaN + HCl + H_2 . \tag{1}$$

The second reaction leading also to the deposition of GaN is [8 to 10]

$$\left.\begin{aligned} 3\,GaCl + 2\,NH_3 &\rightarrow 2\,GaN + GaCl_3 + 3\,H_2 , \\ GaCl_3 + NH_3 &\rightarrow GaCl_3 \cdot NH_3 \rightarrow GaN + 3\,HCl . \end{aligned}\right\} \tag{2}$$

The relative weight of the reactions (1) and (2) depends on the concentrations of NH_3 and GaCl in the reaction chamber [8, 9]. The chemical reactions which lead to the deposition of AlN in the chloride system have not been investigated in detail so far. However, from the results of [4, 11, 12] it may be concluded that the main reaction leading to the deposition of AlN is the decomposition of an $AlCl_3 \cdot xNH_3$ ($1 \leqq x \leqq 3$) complex which is similar to reaction (2) for GaN. Thus, it can be expected that the relative weight of the reactions (1) and (2) for GaN may be of some influence on the deposition and the properties of $Al_xGa_{1-x}N$ layers.

To clear this point two sets of growth experiments were made. In a first series of experiments the conditions were analogous to those for GaN. The flow rates of the gases were constant during growth with typical values of 1 l/min for N_2, 3 ml/min for HCl, and 850 ml/min for NH_3, which corresponds to the optimum growth conditions for GaN [13]. In a second series of experiments a largely enhanced HCl flow rate was used during the first stage of the growth process which leads to an increased influence of reaction (2) on the nucleation of the layers. In both cases the growth experiments were started with GaN, then $Al_xGa_{1-x}N$ layers with rising Al content were grown by increasing the temperature of the Al source in the range from 600 to 750 °C. Some preliminary attempts were made to dope the layers with zinc.

In some cases indications were found that an intermediate liquid phase is formed during the crystallization process. Thus, it seems to be possible that the growth is due to the vapour–liquid–solid mechanism under certain conditions. Systematic investigations in this direction are now in progress and will be published at a later date.

2.2 Measurements

The Al content of the layers was estimated by energy dispersive X-ray microanalysis (EDAX) using Al K and Ga L radiation. The mole fraction x was calculated from the measured intensity values using standards with x values outside those of the samples and correcting the calibration curves for absorption influences. No exact ZAF correction was made. To examine the homogeneity of the layers perpendicular to the surface two sets of measurements with different accelerating voltages were made.

The structural characterization of the layers was performed by RHEED investigations. Charging effects were avoided with the aid of an auxiliary electron gun. Scanning electron microscope studies of the surface morphology of the layers were also performed.

Conductivity type, carrier concentration, and carrier mobility of the layers were determined in the temperature range from 77 to 300 K by Hall effect and resistivity measurements using the van der Pauw method [14]. Ohmic contacts could be prepared in the same manner as for GaN [15].

Optical transmission measurements were made in a conventional double-beam arrangement in the photon energy range from 1.8 to 3.65 eV. No attempts were made to calculate the absorption coefficient of the layers because of the large uncertainties concerning the necessary corrections due to reflection, surface roughness, and possible interference effects. Photoluminescence measurements were performed at room temperature and near 80 K at nitrogen laser excitation.

3. Results and Discussion

3.1 Composition and structural properties

Under the chosen growth conditions $Al_xGa_{1-x}N$ layers with Al contents up to $x = 0.45$ were obtained. All layers showed good lateral homogeneity with a weak perpendicular composition gradient with the higher Al content on the top of the layers. Furthermore, it was found that all of the investigated samples contain a considerable amount of silicon (up to 1.5%). No relation between the Al and the Si contents of the layers was observed.

Table 1

Orientation relations for $Al_xGa_{1-x}N$ on sapphire

substrate orientation	orientation relations $Al_xGa_{1-x}N$/sapphire
(0001)	(0001) || (0001)
	[10·0] || [1$\bar{1}$·0]
(1$\bar{1}$02)	(11$\bar{2}$0) \|\| (1$\bar{1}$02)
	[00·1] || [$\bar{1}$1·1]
(10$\bar{1}$0)	(11$\bar{2}$0) \|\| (10$\bar{1}$0)*)
($\bar{1}$011)	(11$\bar{2}$1) \|\| ($\bar{1}$011)*)
	(11$\bar{2}$4) \|\| ($\bar{1}$011)*)

*) Other relations were observed, too.

As it follows from the RHEED investigations epitaxial growth takes place on (0001)- and (1$\bar{1}$02)-oriented substrates whereas films on (10$\bar{1}$0)- and ($\bar{1}$011)-oriented substrates were polycrystalline with large crystallites in various preferred orientations. However, no ring patterns were observed. All layers showed wurtzite structure as expected from the structure of GaN and AlN [16]. The orientation relations are compiled in Table 1. They were found to be independent of the composition of the layers. On the (10$\bar{1}$0)- and ($\bar{1}$011)-oriented substrates also other not indexed orientation relations occurred. The orientation relations for the (0001)- and (1$\bar{1}$02)-oriented substrates are in agreement with earlier studies of epitaxial GaN [17, 18] and AlN [19] on sapphire. Contrary to the results of [17] for Mg-doped GaN no influence of Zn doping on the orientation relations could be observed. Above, the structural perfection seems to be independent of the Zn doping. Both statements are reasonable in view of the nearly equal covalent radii of Ga, Al, and Zn [20].

RHEED patterns of films on (0001)-oriented substrates showed in some cases diffraction maxima elongated towards the shadow edge which is characteristic of electron diffraction at surfaces having large smooth areas [21]. Corresponding RHEED pat-

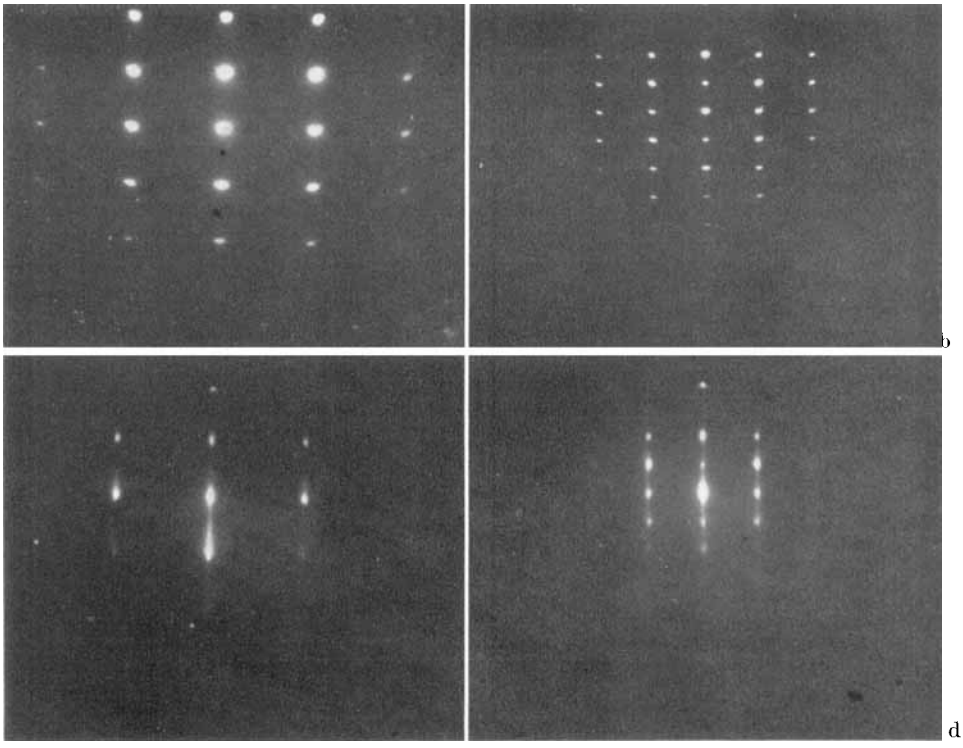

Fig. 1. RHEED patterns of $Al_xGa_{1-x}N$ layers on (0001)-oriented sapphire substrates for the azimuths a), c) [1$\bar{1}$·0] and b), d) [01·0] for layers with a), b) high, and c), d) relatively low surface roughness

terns for the azimuths [01·0] and [1$\bar{1}$·0] are shown in Fig. 1. Besides the spot elongation diffuse streaks of low intensity were observed in some other samples which are caused by stacking faults in the [00·1] growth direction. However, a correlation between the occurrence of stacking faults and surface roughness could not be found.

In a few cases maxima of low intensity could be observed in the [00·1] direction. This result can be interpreted by the occurrence of a stacking sequence corresponding to the cubic sphalerite structure with twinning. Diffuse streaks of negligible intensity corresponding to the other ⟨111⟩ directions of the cubic structure were observed only occasionally. Thus, the low tendency of GaN to crystallize in the cubic sphalerite structure [22] exists also in the $Al_xGa_{1-x}N$ mixed crystals in the considered composition range.

Diffraction patterns of films having low surface roughness showed Kikuchi diagrams of low intensity (Fig. 2). Although RHEED diagrams as shown in Fig. 1 were found for all compositions investigated, Kikuchi bands could be observed only up to $x \approx 0.1$, which indicates that the structural perfection of the layers decreases slowly with rising Al content.

Surface morphology studies of epitaxial films on (0001)-oriented substrates showed that the shape of the surface depends strongly on the growth conditions and the substrate preparation. It was found that layers grown with an enhanced HCl flow rate during the nucleation stage are smoother which seems to be in accordance with some recently published results for GaN [18]. Characteristic of most of the samples is the

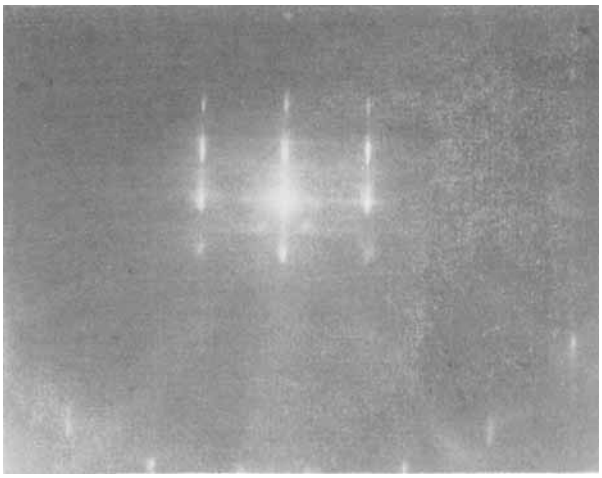

Fig. 2. RHEED pattern of an $Al_xGa_{1-x}N$ layer showing Kikuchi diagram (substrate orientation (0001), azimuth [1$\bar{1}$·0], accelerating voltage 65 kV)

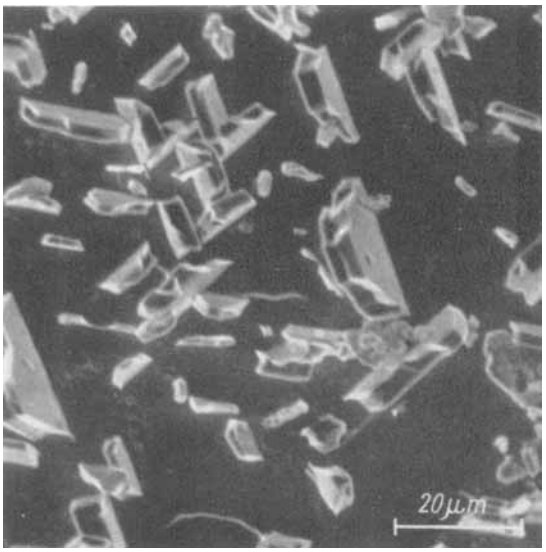

Fig. 3. Micrograph of a smooth $Al_{0.15}Ga_{0.85}N$ epitaxial layer with single crystal platelets in twin position on the top

presence of small individual crystals with diameters up to 20 µm on the top of the layer which originate in the last growth stage. These crystals seem to be oriented in six preferred directions, probably (30$\bar{3}$4) twins (Fig. 3). Some samples showed signs of an etching or dissolution process on the surface. In these cases the individual crystals are absent. Generally, it was found that the perfection of the layers decreases with rising Al content which is in agreement with the RHEED measurements.

3.2 Electrical properties

All undoped $Al_xGa_{1-x}N$ samples showed n-type conductivity with electron concentrations n and mobilities μ independent of temperature in the range from 77 to 300 K. The composition dependence of n and μ is shown in Fig. 4 and 5, respectively. Although there is some scattering in the n values the tendency to lower electron concentrations with rising Al content is clearly pronounced (Fig. 4). However, the electron concentration is rather high even in the samples with the highest x values which seems to be in contradiction to the fact that undoped AlN grown with the same technique is known

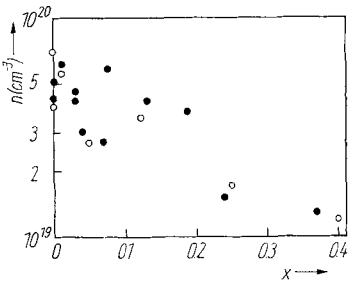

Fig. 4. Composition dependence of the electron concentration for samples grown under usual conditions (○) and with an enhanced HCl flow rate during nucleation (●)

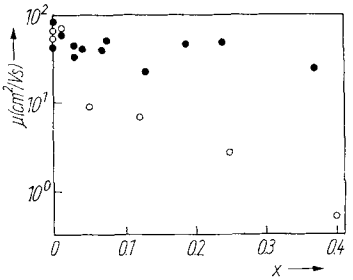

Fig. 5. Composition dependence of the electron mobility for samples grown under usual conditions (○) and with an enhanced HCl flow rate during nucleation (●)

to be a high-resistivity material [12]. There are two possible explanations for this result. Firstly, it is possible that the defect mechanism leading to the high electron concentrations in GaN is also acting in $Al_xGa_{1-x}N$ up to at least $x \approx 0.45$. Secondly, the high n values may be caused by the relatively high Si content of the layers because Si is known to be a donor in AlN [4]. To decide between these two possibilities it would be necessary to grow $Al_xGa_{1-x}N$ films with largely reduced Si content. No influence of the growth conditions on the electron concentration was found.

As it can be seen from Fig. 5 an enhanced HCl flow rate during the nucleation process of the layers leads to higher mobilities than under usual nucleation conditions. This may be caused either by a higher microscopic perfection of the layers in the mixed crystal region (this point of view is supported by the surface morphology studies) or by a lower degree of compensation. Extrapolating the highest measured mobility values over the whole mixed crystal range, an electron mobility of $\mu \geqq 10$ cm²/Vs is expected in AlN for carrier concentrations of about 10^{19} cm^{-3}. This value is much higher than the only published mobility of 1 to 3 cm²/Vs for high-resistivity n-type AlN single crystals [23]. At present, no complete quantitative calculation of the electron mobility in AlN can be made because of the lack of experimental information on many material parameters needed in mobility evaluations. A rough estimate of the electron mobility including scattering by polar optical phonons, piezoelectric scattering, and ionized impurity scattering using phonon data from [24], elastic and piezoelectric constants from [25], an effective mass of $m/m_0 = 0.33$ (estimated on the basis of a two-band approximation and accounting for the trends in the conduction band effective masses of wurtzite-type compounds [26]), and the mobility relations for wurtzite-type compounds from [27] yields a lattice mobility of about 400 cm²/Vs at room temperature and a mobility of about 25 cm²/Vs for $n = 10^{19}$ cm^{-3} and a degree of compensation of 0.7 typical for our GaN samples (estimated according to [27]). The latter value is in rather good agreement with the extrapolated mobility for AlN if we take into account that scattering by acoustic phonons, nonpolar optical phonons, neutral impurities, and other types of possible defects are neglected in our estimation. Obviously, the low mobility value found in [23] is connected with band tail conduction effects due to high compensation [28].

Attempts to measure the electrical parameters of the Zn-doped samples were not successful because of sample inhomogeneities.

3.3 Optical properties

In all investigated samples a strong decrease of transmission was observed around 3.5 eV. For samples with good crystalline perfection a clear connection between Al

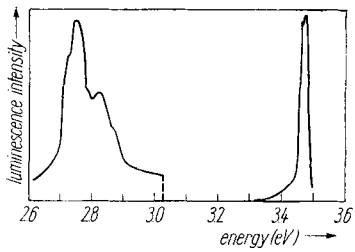

Fig. 6. Typical luminescence spectrum of a Zn-doped $Al_xGa_{1-x}N$ layer ($x \approx 0.1$, $T = 293$ K)

content and the onset of appreciable transmission was found which shows the expected increase of the band gap with rising x. Some samples (especially all Zn-doped samples) exhibit a structureless transmission spectrum which points to the predominant influence of scattering and/or composition inhomogeneities perpendicular to the sample surface.

The luminescence spectra of undoped samples are dominated by a structure at 3.46 eV. In accordance with a remark in [29] on the luminescence spectra of Al-implanted GaN (up to 10% Al) we note the intricate fact that the energy of this structure seems to be independent of x up to about $x = 0.3$, although the transmission measurements show the expected increase of the band gap. If we assume that in analogy to GaN [1, 30] the 3.46 eV line is due to the annihilation of an exciton bound to a donor and that the exciton binding energy is not essentially changed with composition the observed behaviour points to a donor level which remains fixed relative to the valence band. Such types of electron levels have been recently found in $Al_xGa_{1-x}As$ [31] and have been ascribed to lattice vacancies the wave functions of which are made up primarily of valence-band wave functions.[1]) It is not out of the way to interpret our results in the same manner because the dominant donor in undoped GaN is believed to be a nitrogen vacancy [30]. May be, that the uncleared divergence in the temperature dependence of some luminescence bands and the band gap in GaN [30, 33, 34] can be explained on the basis of similar models.

The luminescence spectra of the Zn-doped samples showed in addition to the 3.46 eV line a broad donor–acceptor like structure near 2.8 eV (Fig. 6), obviously caused by a Zn-induced acceptor [1]. In some cases we observed a further broad structure near 2.2 eV. A similar structure uncleared in origin is known also in GaN [35 to 37]. Nothing can be said about the composition dependence of these two levels because of the large sample inhomogeneities found not only in the electrical and the optical transmission measurements but also in the luminescence investigations.

4. Conclusions

Up to now, the $Al_xGa_{1-x}N$ layers obtained do not fulfil the main demand on a material for light-emitting diodes because all layers showed n-type conduction with unexpected high electron concentrations even at the highest Al contents investigated. The influence of Zn doping on the electrical properties could not be established because of large inhomogeneities in the doped samples. Obviously, further improvements in the growth technique, an extension of the experiments over the whole composition range, and may be, the use of other acceptor impurities are necessary to verify the supposed possibility of amphoteric doping in this system or at least to understand its impossibility.

[1]) For the intricate and widely unknown properties of vacancy states, even in the best known semiconductor Si, see e.g. [32].

Acknowledgements

The authors are indebted to Prof. Dr. H. Berger and Prof. Dr. G. O. Müller for encouraging discussions and to Mr. W. Boutin, Mrs. E. Hähnlein, Mrs. K. Hagenstein, Mrs. E. Kramer, and Mr. G. Matzkeit for technical assistence in the sample preparation, RHEED investigations, electrical and optical measurements, respectively.

References

[1] J. I. Pankove, S. Bloom, and G. Harbeke, RCA Rev. **36**, 163 (1975).
[2] R. Madar, G. Jacob, J. Hallais, and R. Fruchart, J. Crystal Growth **31**, 197 (1975).
[3] U. V. Desnica, N. B. Urli, and B. Etlinger, Phys. Rev. B **15**, 4119 (1977).
[4] G. A. Slack and T. F. McNelly, J. Crystal Growth **34**, 263 (1976).
[5] R. F. Rutz, Appl. Phys. Letters **28**, 379 (1976).
[6] B. Baranov and L. Däweritz, phys. stat. sol. (a) **38**, K111 (1976).
[7] B. Baranov, H. Neumann, and H.-G. Ernst, Kristall und Technik **12**, K18 (1977).
[8] V. S. Ban, J. Electrochem. Soc. **119**, 761 (1972).
[9] A. Shintani and S. Minigawa, J. Crystal Growth **22**, 1 (1974).
[10] L. A. Marasina and I. G. Pichugin, Izv. Akad. Nauk SSSR, Ser. neorg. Mater. **12**, 2054 (1976).
[11] A. J. Noreika and D. W. Ing, J. appl. Phys. **39**, 5578 (1968).
[12] W. M. Yim, E. J. Stofko, P. J. Zanzucchi, J. I. Pankove, M. Ettenberg, and S. L. Gilbert, J. appl. Phys. **44**, 292 (1973).
[13] I. G. Pichugin and M. Tlachala, Izv. Akad. Nauk SSSR, Ser. neorg. Mater. **12**, 2051 (1976).
[14] L. J. van der Pauw, Philips Res. Rep. **13**, 1 (1958).
[15] H. Neumann, W. Seifert, M. Staudte, and A. Zehe, Kristall und Technik **9**, K69 (1974).
[16] H. Schulz and K. H. Thiemann, Solid State Commun. **23**, 815 (1977).
[17] M. Sano and M. Aoki, Japan. J. appl. Phys. **15**, 1943 (1976).
[18] R. Madar, D. Michel, G. Jacob, and M. Boulou, J. Crystal Growth **40**, 239 (1977).
[19] M. T. Duffy, C. C. Wang, G. D. O'Clock, S. H. McFarlane, and P. J. Zanzucchi, J. elektron. Mater. **2**, 359 (1973).
[20] J. A. van Vechten and J. C. Phillips, Phys. Rev. B **2**, 2160 (1970).
[21] D. W. Pashley, Adv. Phys. **5**, 173 (1956).
[22] W. Seifert and A. Tempel, phys. stat. sol. (a) **23**, K39 (1974).
[23] J. Kubatova, J. Pastrnak, and V. Zelezny, Proc. Conf. Mixed Crystals 1975, Reinhardsbrunn 1975 (p. 119).
[24] A. T. Collins, E. C. Lightowlers, and P. J. Dean, Phys. Rev. **158**, 833 (1967).
[25] Landolt-Börnstein, Zahlenwerte und Funktionen aus Naturwissenschaft und Technik, Neue Serie, Band III/2, Hrsg. K.-H. Hellwege und A. M. Hellwege, Springer-Verlag, Berlin-Heidelberg-New York 1969.
[26] M. Cardona, J. Phys. Chem. Solids **24**, 1543 (1963).
[27] H. Neumann, Kristall und Technik **12**, 961 (1977).
[28] D. Redfield, Adv. Phys. **24**, 463 (1975).
[29] J. I. Pankove and J. A. Hutchby, J. appl. Phys. **47**, 5387 (1976).
[30] J. I. Pankove, J. Lum. **7**, 114 (1973).
[31] D. V. Lang, R. A. Logan, and L. C. Kimerling, Proc. XIII. Internat. Conf. Phys. Semicond., Rome 1976.
[32] S. G. Louie, M. Schlüter, J. R. Chelikowsky, and M. L. Cohen, Phys. Rev. B **13**, 1654 (1976).
[33] E. Ejder and H. G. Grimmeis, Appl. Phys. **5**, 275 (1974).
[34] M. Aoki, M. Sano, and T. Ogino, Ann. Rep. Engng. Res. Inst. Fac. Sci. Univ. Tokyo **34**, 125 (1975).
[35] A. M. Zykov and G. K. Gaido, Fiz. Tekh. Poluprov. **6**, 185 (1972).
[36] J. I. Pankove, E. A. Miller, and J. E. Berkeyheiser, J. Lum. **6**, 54 (1973).
[37] L. A. Marasina, I. G. Pichugin, Yu. M. Suleimanov, and S. I. Teslenko, Fiz. Tekh. Poluprov. **8**, 1826 (1974).

(Received July 31, 1978)